Theor Appl Climatol (2012) 109:253–259
DOI 10.1007/s00704-011-0579-5

ORIGINAL PAPER

On the climate response to zero ozone

Isabella Bordi · Klaus Fraedrich · Alfonso Sutera · Xiuhua Zhu

Received: 12 July 2011 / Accepted: 22 December 2011 / Published online: 10 January 2012
© Springer-Verlag 2012

Abstract Although ozone appears in the Earth's atmosphere in a small abundance, it plays a key role in the energy balance of the planet through its involvement in radiative processes. Its absorption of solar radiation leads to the temperature increase with height defining the tropopause and the stratosphere. Moreover, excluding water vapor, O_3 is the third most important contributor (after CO_2 and CH_4) to the greenhouse radiative forcing. Thus, the total removal of O_3 content in an Earth-like atmosphere may cause interesting response of the climate system that deserves further investigation. The present paper addresses this issue by means of a global climate model where the atmosphere is coupled with a passive ocean of a given depth. The model, after reaching the statistical equilibrium under present climate conditions, is perturbed by a sudden switch off of the O_3 content. Results obtained for the new equilibrium suggest that the model gets in a colder state mainly because of the water vapor content decrease. Most of the cooling occurs in the Southern Hemisphere while in the Northern Hemisphere the ice cap melts quite consistently. This process appears to be governed by the northward cross-equatorial heat transports induced by changes in the general circulation.

1 Introduction

The Earth's radiative budget depends on many variables including the noncondensing greenhouse gases, the atmospheric water content in all its phases, and the ocean heat storage. The latter depends on whether the sea surface is covered by ice; in this case, the ocean heat intake reduces to a residual transport due to molecular diffusion. Also water vapor, being its source the evaporation of the ocean water, depends on the ice coverage and the associated insulating effect (Saltzman and Sutera 1984). CO_2 and O_3 concentrations, instead, have no direct dependence on the surface state; therefore, they are the obvious parameters to perturb when the climate response to variations of the radiative forcing is studied.

The recent interest on the future climate in relation to an increasing CO_2 concentration has prompted a staggering number of studies on the response that the climate system might have to the expected changes of this greenhouse gas. In that framework, the O_3 variations have been considered mainly for their effect on the ultraviolet screen of sunrays with very minor concern on the radiation budget. IPCC (2007) estimated that the observed variations of O_3 concentration have contributed to the radiation budget about 0.3 Wm^{-2} due to its increase near the tropopause, and −0.1 Wm^{-2} due to its decrease in the stratosphere. These modest contributions, with respect to a total of 3.2 Wm^{-2} due to the other gases, lead to neglect at the first order the effect of this species on climate. However, the complete removal of O_3 may cause a more interesting response since this gas is active both in the solar and the terrestrial spectrum of the radiation. Without ozone, in fact, more solar radiation should reach the surface but, at the same time, more terrestrial radiation would leave the planet. The balance of these competing effects may produce a net cooling or heating in the system, driving the climate either way (see Ramanathan and Dickinson 1979 for an in-depth analysis).

At present day conditions, in the stratosphere, the absorption of solar and infrared radiation of this gas exceeds the emission by 15 Wm^{-2}, leading to a net warming that is

I. Bordi (✉) · A. Sutera
Department of Physics, Sapienza University of Rome, Rome, Italy
e-mail: isabella.bordi@roma1.infn.it

K. Fraedrich · X. Zhu
KlimaCampus, Universität Hamburg, Hamburg, Germany

balanced by CO_2 and H_2O cooling. The removal of ozone would result in a temperature decrease of several degrees per day high up in the atmosphere. Then, it would cause a major change of the stratospheric energy balance leading to a colder stratosphere, because only CO_2 and H_2O will be left to balance solar fluxes. It is foreseeable that, in such a circumstance, the tropopause height will rise, leading to a further cooling. In the polar atmosphere, this response may induce a surface cooling and the formation of sea ice with a drastic loss of water vapor supply. Given that the Southern Hemisphere (SH) has a very small percentage of land compared with the Northern Hemisphere (NH), the cooling may imply a freeze of a large fraction of the southern hemisphere ocean. Such an effect should be less pronounced in the NH. In this case, a strong pole-to-pole surface temperature gradient will be established with strong cross-equatorial heat fluxes leading to a warming of the NH. Following this reasoning, it remains to see whether these heat transports can have an effect large enough to influence the NH polar cap. On first instance, this possibility cannot be ruled out. Arguments based on Budyko–Sellers energy balance models (Lindzen 1990) suggest, in fact, that, by increasing the ice extension, heat fluxes raise the temperature of the ice-free regions. In this framework, we should expect that the SH, due to its large fraction of ocean coverage, should efficiently respond to the radiative perturbation, while the NH should be less sensitive to it. Thus, if our reasoning holds, we would observe that while the SH cools, the NH should warm.

In the present paper, these questions are investigated by means of a global climate model (GCM) where the atmosphere

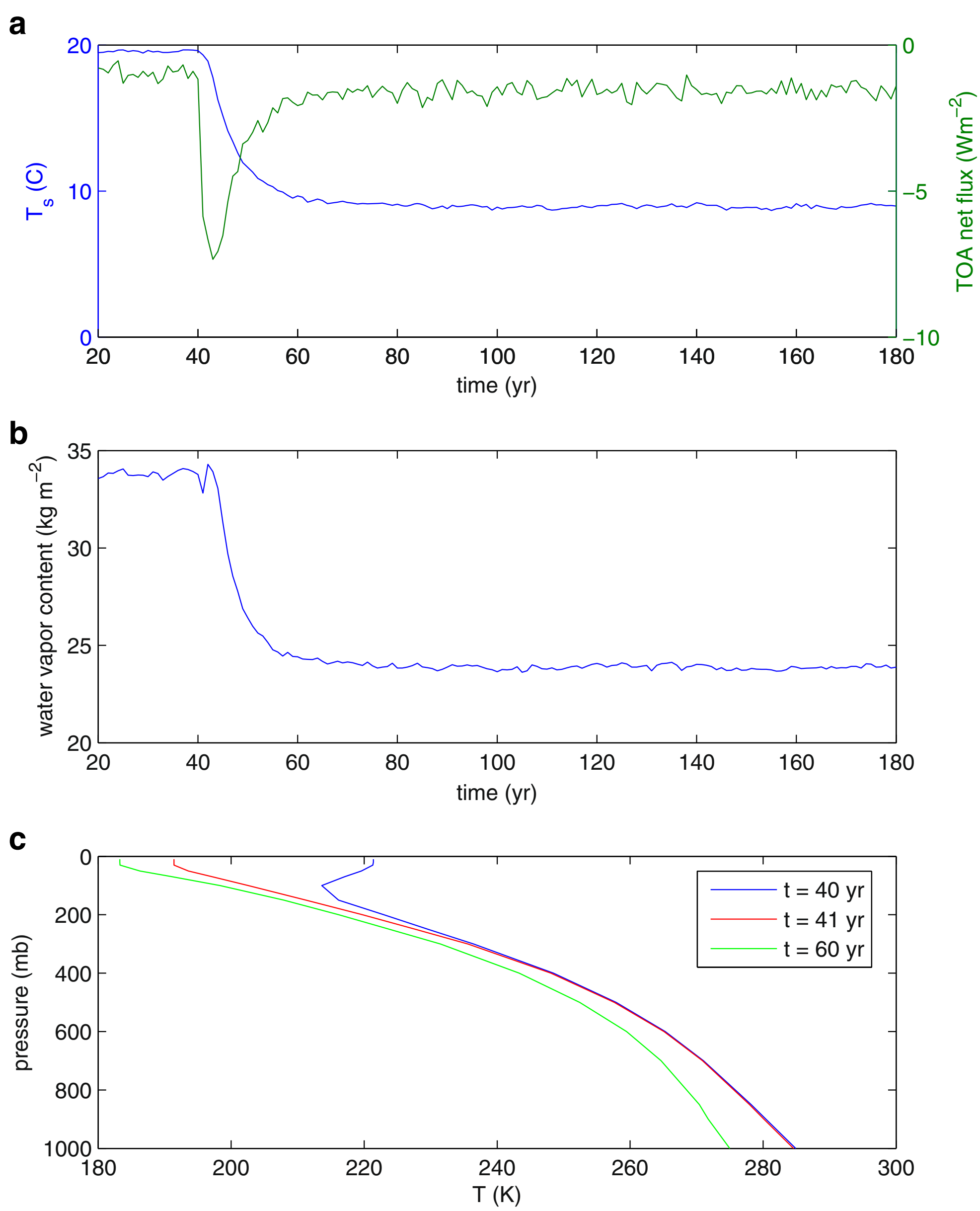

Fig. 1 Global mean (area weighted) **a** time evolution of TOA net flux (*green line*) surface temperature (*blue line*) and **b** water vapor content; **c** global mean vertical temperature profile at $t=$ 40 years (*blue*), $t=41$ years (*red*), and $t=60$ years (*green*)

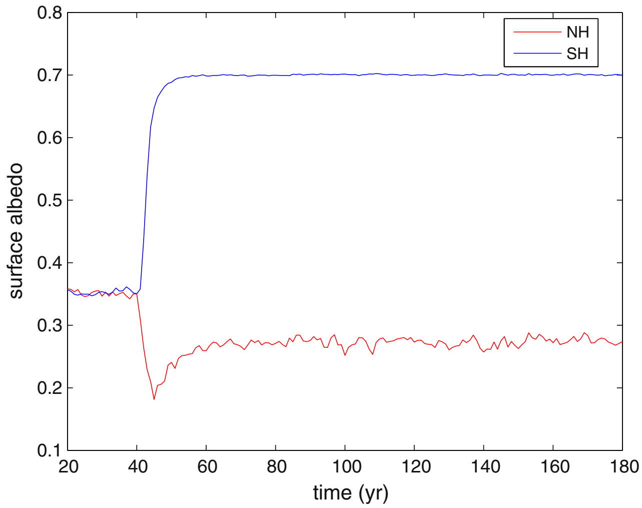

Fig. 2 Time evolution of surface albedo in NH [*red*, averaged between (47°, 86°)] and SH [*blue*, averaged between (−47°, −86°)]

is coupled with a passive ocean of a given depth. The model, after reaching the statistical equilibrium for present climate conditions, is perturbed by a sudden switch to zero of the ozone content, and then, it is left to evolve towards its new equilibrium. A description of the ensuing general circulation is presented. Few conclusions and speculations are offered in the final section.

2 A planet simulator

Analyses are performed using the portable global climate model Planet Simulator (PlaSim, freely available under http://www.mi.uni-hamburg.de/plasim where additional information about the model can be found; Fraedrich et al. 2005). The model is a coupled ocean–sea ice–atmosphere GCM at a low spatial resolution (T21) with 17 sigma levels. Land distribution is Earth-like with no land glaciers forming. The noncondensing greenhouse gases are limited to CO_2 and O_3. While the former is well mixed through the model's atmospheric column, the O_3 profile is prescribed following the analytic distribution of Green (1964):

$$u_{O_3}(z) = \frac{a + ae^{-b/c}}{1 + e^{(z-b)/c}}, \tag{1}$$

where $u_{O_3}(z)$ is the ozone amount (in centimeters STP) in a vertical column above the altitude z, a is the total ozone amount in a vertical column above the ground, and b the

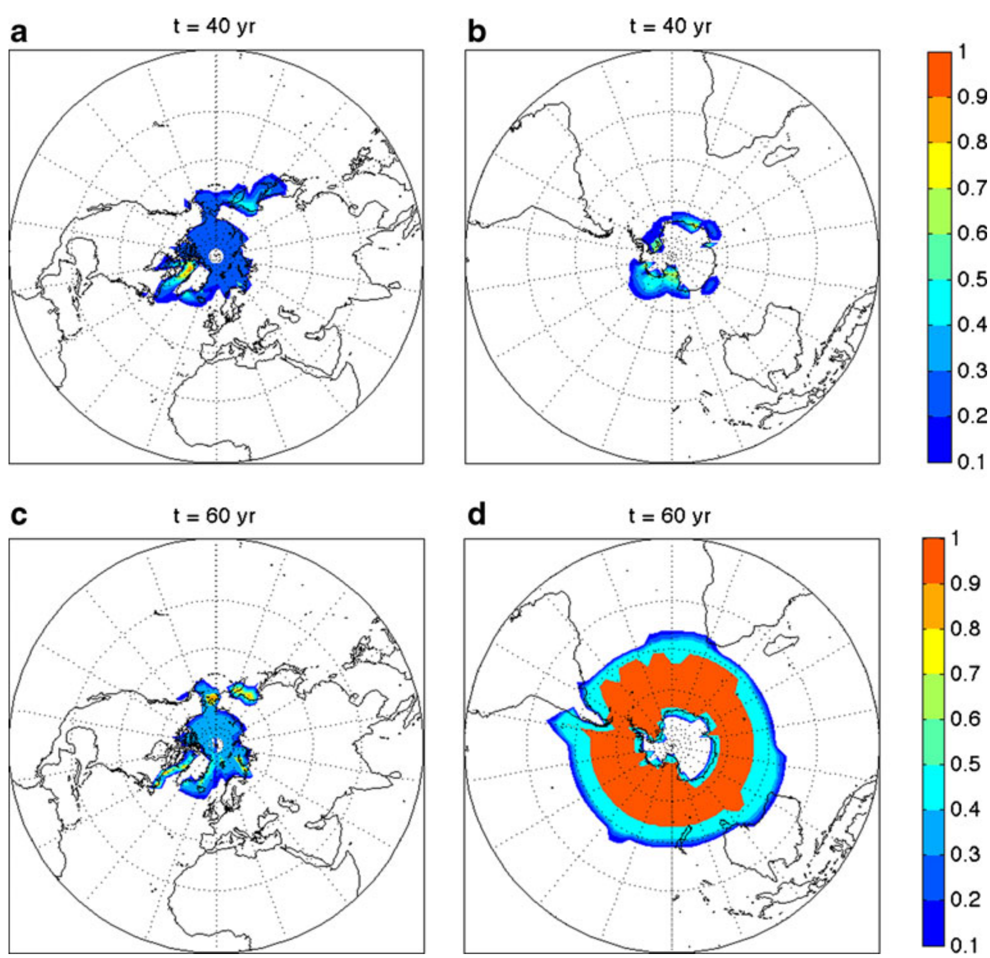

Fig. 3 Sea ice cover (fraction) at t=40 in **a** NH and **b** SH, and at t=60 years in **c** NH and **d** SH

altitude at which the ozone concentration has its maximum. Setting a=0.4 cm, b=20 km, and c=5 km, (1) fits closely the mid-latitude winter ozone distribution. The annual cycle and the latitudinal dependence is introduced by varying a with time t and latitude ϕ as:

$$a(t, \phi) = a_0 + a_1 \cdot |\sin(\phi)| + a_c \cdot \sin(\phi) \cdot \cos(2\pi(d - d_{\mathrm{off}})/\mathrm{ndy}), \tag{2}$$

where d is the actual day of the year, d_{off} an offset, and ndy the number of days per year. The defaults of the involved parameters are: a_0=0.25, a_1=0.11, and a_c=0.08.

The short wave radiation scheme is based on Lacis and Hansen (1974) for the cloud-free atmosphere. For the cloudy part, either constant albedos and transmissivities for high-, middle- and low-level clouds may be prescribed, or parameterizations following Stephens (1978) and Stephens et al. (1984) may be used (default setup). The transmissivities for water vapor, carbon dioxide, and ozone are taken from Sasamori (1968).

3 Results

The model is run first with the nominal present concentrations of the greenhouse gases (carbon dioxide and ozone), and the ocean depth is set to 50 m. It turns out that the statistical equilibrium is reached after 40 years; thereon, O_3 concentration is set to zero. The new equilibrium state settles after 40–50 years.

In Fig. 1 we illustrate the sequence of events that are occurring in the model on yearly basis. The initial global radiative imbalance at the top of the atmosphere (TOA) induced by the ozone removal is about −8 Wm^{-2} (green curve in Fig. 1a at time 41 years). This amount does not justify the 13 C drop in the global mean surface temperature observed later on (blue curve in Fig. 1a). However, by inspecting the atmospheric water content, we notice a decrease of about 30% (Fig. 1b) by year 60 that induces an additional 30–40 Wm^{-2} in energy lost by the system. This response is a consequence of the drastic change in the stratospheric temperature profile (Fig. 1c) occurring between year 40 (blue line) and 41 (red line). After the time of the switch off, the decline of the air

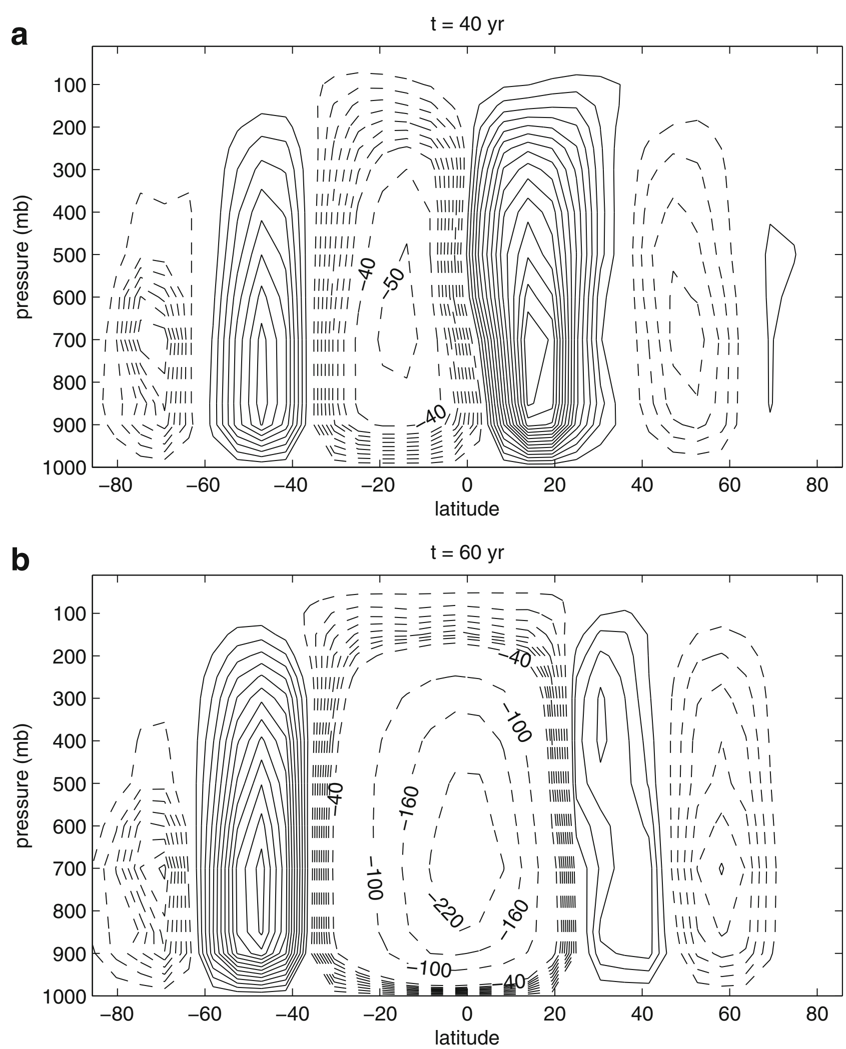

Fig. 4 Latitude–height (*pressure*) cross-section of the mass stream function for **a** t=40 years and **b** t=60 years. Units are in 10^9 kg s^{-1}, contours are every 4×10^9 kg s^{-1} within the range (−32, 60) and the zero line is excluded; values less than -40×10^9 kg s^{-1} are shown with labels. *Solid lines* denote clockwise circulation

temperature appears to become large and robust even at the surface (green line). Thus, there is a global response to the imposed O_3 change that is magnified by the induced water vapor reduction. However, this does not exhaust the peculiarities of the climate response; in particular, there is an inter-hemispheric asymmetry, which is worth illustrating.

Let us consider, for instance, the surface albedo averaged around the two polar caps [(47°, 86°) for NH, and (−47°, −86°) for SH]. Their yearly mean behavior is shown in Fig. 2. In the SH (blue curve), at the time of the switch off (t=41 years), the albedo jumps to values typical for ice, remaining constant thereon. At the same time, in NH (red curve), the albedo decreases reaching a new asymptotic state at a lower value with respect to that of the control run. This corresponds to a sudden sea ice increase in SH, while in the NH just the reverse occurs. Also, it should be noted that in the NH, there is a transient behavior where the albedo dips down even further than the asymptotic value reached 20 years later from the switch off. This effect resembles the phenomenon known as small ice cap instability that disallows polar ice caps smaller than a certain critical size determined by heat diffusion and radiative damping (see for example Lee and North 1995 and references therein). In both hemispheres, the time scale to reach the new equilibrium is essentially dictated by the ocean heat capacity, and it would be easy to prove that it is longer for a deeper ocean.

To better illustrate this inter-hemispheric asymmetry, we plot the spatial distribution of sea ice cover for t=40 years (Fig. 3a) and for t=60 years (Fig. 3b). It can be noted that at t=40 years, the area extension of sea ice is larger in the NH than in the SH, while at t=60 years the opposite occurs (the NH enjoys an almost free polar cap and the SH is in a deep freeze). This means that, in accounting for this behavior, heat and water vapor have to be transported across the equator, and as a consequence, we should expect a significant modification of the general circulation of the atmosphere. Our guess is supported by the following analysis.

Hadley cell In the SH the Hadley cell is strongly intensified and penetrates deep into the NH, while in the NH a weaker Hadley cell is shifted poleward (Fig. 4). The Ferrel cells intensify in both hemispheres, in particular in the SH, while in the NH it is displaced northward. In the NH the polar cell almost disappears, while in the SH it remains. Note that in Bordi et al. (2004, 2007) this type of behavior has been theoretically investigated for Eady modes in presence of a stratosphere and for a GCM with Newtonian cooling.

Heat transports Figure 5 shows the time behavior of the meridional heat transports (vT, with v the meridional velocity and T the temperature) vertically integrated over the lower levels between 850 and 1,000 mb, for the sample latitudes of 19.4° and −19.4°. Consistent with the Hadley cells displayed before, the heat transports in the NH change from equatorward to poleward after zeroing out the ozone content. In the SH, instead, they remain equatorward but they are intensified. It is worth noting that the initial pole-to pole surface temperature gradient (not shown) is about 20 K at year 40, and it quickly increases to about 60 K after the ozone is switched off due to the inter-hemispheric asymmetry of sea ice extension.

So far, we have discussed the response of a global circulation model, which simulates an Earth-like planet and it would be impossible to translate our results to the true Earth. Nevertheless, some consideration is allowed. In the real

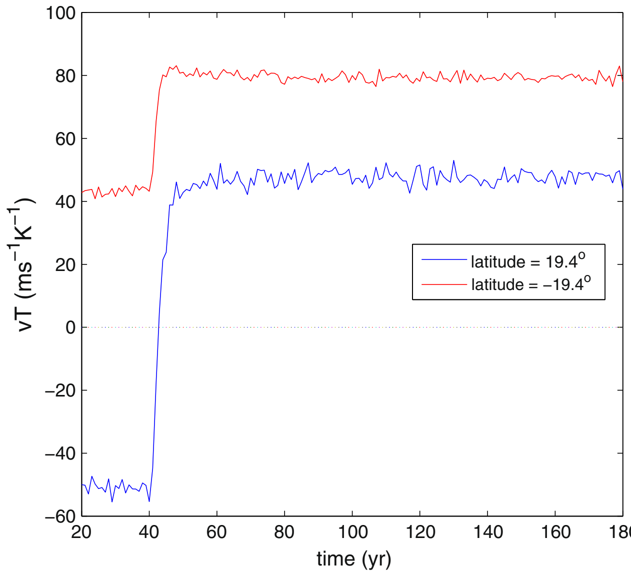

Fig. 5 Time evolution of zonal mean meridional heat transports (vT) vertically integrated over (850, 1,000) mb and normalized by p_0= 1,000 mb for two sample latitudes, north (*blue*) and south (*red*) of the equator

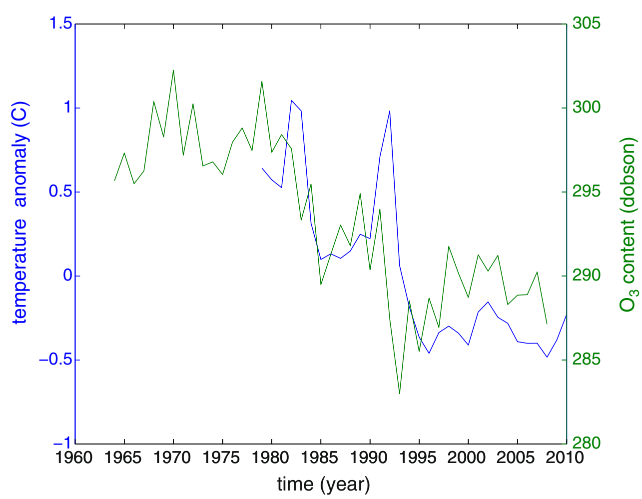

Fig. 6 Stratospheric temperature anomaly (*blue*) and ozone content averaged over the latitude range (−60°, 60°; *green line*)

world, ozone content is about 300 Dobson. Its variability is far from being constant, though its fluctuations are, on the global scale, small and confined to several Dobson. Just to get an idea of these fluctuations, it is worthwhile to plot the few data available (see Fig. 6). The green curve (left y-axis) shows the decline of the total ozone content, while the blue curve (right y-axis) the stratospheric temperature anomaly retrieved from MSU/AMSU datasets (Christy et al. 2007). Apart of the two peaks registered in the temperature anomaly time series (that are associated with two major volcanic explosions), the decline of the two curves appears similar.

On these grounds, it may be speculated that an inter-hemispheric asymmetry should be observed: part of the recently observed surface temperature change in the NH might be related to the decline of the ozone content. However, to be consistent with our analysis, we should observe an increasing of sea ice extension in the SH and a decline in NH. Given the observed modest ozone changes, it appears that the detection of such a contribution can be hardly determined.

4 Conclusions

In the present paper, we have investigated the effects of removing ozone content from a global climate model simulating an Earth-like condition. It has been found that the model attains a new colder state mainly because of the water vapor content decrease. There are interesting features to be noted:

- Most of the cooling occurs in the SH while the NH warms so that its ice cap melts quite consistently. This process is governed by northward cross-equatorial heat transports that provide the heat required for the melting;
- The SH Hadley cell penetrates deep into the NH, while in the NH, a weaker Hadley cell is displaced poleward. The Ferrel cells intensify in both hemispheres, especially in SH, while it is displaced northward in the NH. The polar cell in NH almost disappears, while in the SH remains; and
- Despite the modest ozone decline recently observed (WMO 2011), we speculate that its effect on the Earth's climate should be sought in terms of differences in the inter-hemispheric circulation.

It is worth noticing that, in absence of O_3, a modest decrease of CO_2 concentration may easily flip the model climate into a modern snowball Earth state.

The PlaSim, despite some heavy simplifications, especially those concerning the radiative noncondensing species (only CO_2 and O_3 are considered) and the slab ocean, simulates a reasonable present climate. These limitations that may appear as an oversimplification compared with the state-of-the-art GCM, by drastically reducing the parameter space, allow us to isolate the effects of the ozone removal on the thermal structure and general circulation of the atmosphere, which is the aim of the study. However, further analyses are suggested to check the results obtained so far against more complex GCMs that relax many of the simplifications and take into account a full-resolved ocean.

Moreover, in the present paper, the yearly mean fields have been considered to describe the time behavior of the model solutions, neglecting a detailed description of the atmospheric dynamics at the new equilibrium. The thermal structure of the troposphere, since very little solar radiation is absorbed in the troposphere, is maintained by an approximate balance among infrared radiative cooling, vertical transports of sensible and latent heat away from the surface by small-scale eddies, and large-scale heat transports by synoptic-scale eddies. All these contributions should be analyzed and compared with those resulting from the control run to better describe the changes occurring in the atmospheric dynamics. Of particular interest appears to be the analysis of the eddy heat transports induced by the enhanced pole-to-pole temperature gradient. These will be topics of future investigations.

Acknowledgments The ozone data displayed in Fig. 6 have been freely retrieved from the World Ozone and Ultraviolet Radiation Data Centre (WOUDC) from their web site http://www.woudc.org/data/summaries_e.html. Stratospheric temperature anomaly data shown in Fig. 6 have been retrieved from the National Space Science and Technology Center from their web site http://vortex.nsstc.uah.edu. Support by the Max Planck Society is acknowledged (KF).

References

Bordi I, Dell'Aquila A, Speranza A, Sutera A (2004) On the midlatitude tropopause height and the orographic-baroclinic adjustment theory. Tellus 56A:278–286

Bordi I, Fraedrich K, Lunkeit F, Sutera A (2007) Tropospheric double-jets, meridional cells and eddies: a case study and idealized simulations. Mon Weather Rev 135:3118–3133

Christy JR, Norris WB, Spencer RW, Hnilo JJ (2007) Tropospheric temperature change since 1979 from tropical radiosonde and satellite measurements. J Geophys Res 112:D06102. doi:10.1029/2005JD006881

Fraedrich K, Jansen H, Kirk E, Luksch U, Lunkeit F (2005) The planet simulator: towards a user friendly model. Meteorol Zeitschrift 14:299–304

Green AES (1964) Attenuation by ozone and the earth's albedo in the middle ultraviolet. J Appl Opt 3:203–208

IPCC (2007) Climate change 2007—the physical science basis. In: Solomon S, Qin D, Manning M, Chen Z, Marquis M, Averyt KB, Tignor M, Miller HL (eds) Contribution of working group I to the fourth assessment report of the intergovernmental panel on climate change. Cambridge University Press, Cambridge, p 996

Lacis AA, Hansen JE (1974) A parameterization for the absorption of solar radiation in the Earth's atmosphere. J Atmos Sci 31:118–133

Lee W-H, North GR (1995) Small ice cap instability in the presence of fluctuations. Clim Dynam 11:242–246

Lindzen RS (1990) Dynamics in atmospheric physics. Cambrige University Press, p 310

Ramanathan V, Dickinson RE (1979) The role of stratospheric ozone in the zonal and seasonal radiative energy balance of the earth-troposphere system. J Atmos Sci 36:1084–1104

Saltzman B, Sutera A (1984) A model of the internal feedback system involved in late quaternary climatic variations. J Atmos Sci 41:736–745

Sasamori T (1968) The radiative cooling calculation for application to general circulation experiments. J Appl Meteor 7:721–729

Stephens GL (1978) Radiation profiles in extended water clouds. II: parameterization schemes. J Atmos Sci 35:2123–2132

Stephens GL, Ackermann S, Smith EA (1984) A shortwave parameterization revised to improve cloud absorption. J Atmos Sci 41:687–690

WMO (2011) Scientific assessment of ozone depletion: 2010, Global Ozone Research and Monitoring Project—Report No. 52, Geneva, Switzerland, p. 516